


Glycogen Phosphorylase Isoform Regulation of Ventromedial Hypothalamic Nucleus Gluco-Regulatory Neuron 5'-AMP-Activated Protein Kinase and Transmitter Marker Protein Expression

ASN Neuro
Volume 13: 1–14
© The Author(s) 2021
Article reuse guidelines:
sagepub.com/journals-permissions
DOI: 10.1177/17590914211035020
journals.sagepub.com/home/asn



Md. Main Uddin¹, Mostafa M. H. Ibrahim¹ , and Karen P. Briski¹ 

Abstract

Brain glycogen is remodeled during metabolic homeostasis and provides oxidizable L-lactate equivalents. Brain glycogen phosphorylase (GP)-brain (GPbb; AMP-sensitive) and -muscle (GPmm; norepinephrine-sensitive) type isoforms facilitate stimulus-specific control of glycogen disassembly. Here, a whole animal model involving stereotactic-targeted delivery of GPmm or GPbb siRNA to the ventromedial hypothalamic nucleus (VMN) was used to investigate the premise that these variants impose differential control of gluco-regulatory transmission. Intra-VMN GPmm or GPbb siRNA administration inhibited glutamate decarboxylate_{65/67} (GAD), a protein marker for the gluco-inhibitory transmitter γ -aminobutyric acid (GABA), in the caudal VMN. GPbb knockdown, respectively overturned or exacerbated hypoglycemia-associated GAD suppression in rostral and caudal VMN. GPmm siRNA caused a segment-specific reversal of hypoglycemic augmentation of the gluco-stimulatory transmitter indicator, neuronal nitric oxide synthase (nNOS). In both cell types, GP siRNA down-regulated 5'-AMP-activated protein kinase (AMPK) during euglycemia, but hypoglycemic suppression of AMPK was reversed by GPmm targeting. GP knockdown elevated baseline GABA neuron phosphoAMPK (pAMPK) content, and amplified hypoglycemic augmentation of pAMPK expression in each neuron type. GPbb knockdown increased corticosterone secretion in eu- and hypoglycemic rats. Outcomes validate efficacy of GP siRNA delivery for manipulation of glycogen breakdown in discrete brain structures in vivo, and document VMN GPbb control of local GPmm expression. Results document GPmm and/or -bb regulation of GABAergic and nitrergic transmission in discrete rostro-caudal VMN segments. Contrary effects of glycogenolysis on metabolic-sensory AMPK protein during eu- versus hypoglycemia may reflect energy state-specific astrocyte signaling. Amplifying effects of GPbb knockdown on hypoglycemic stimulation of pAMPK infer that glycogen mobilization by GPbb limits neuronal energy instability during hypoglycemia.

Keywords

glycogen phosphorylase-muscle type, glycogen phosphorylase-brain type: insulin-induced hypoglycemia, neuronal nitric oxide synthase, AMPK, corticosterone

Received February 10, 2021; Revised June 13, 2021; Accepted for publication June 27, 2021

Introduction

The brain expends a disproportionate fraction of total body energy to maintain vital high energy-demand nerve cell activities. Iatrogenic insulin (INS)-induced hypoglycemia (IH) is an unremitting complication of obligatory glycemic management of type I diabetes mellitus that poses a risk of neurological impairment and injury (Cryer, 2015, 2017). Hypoglycemic neuro-glucopenia initiates hypothalamus-controlled counter-regulatory autonomic, neuroendocrine, and behavioral outflow that raises blood glucose levels. Dedicated metabolic-sensory neurons in the ventromedial hypothalamic nucleus (VMN) and other select brain loci provide a dynamic cellular

energy readout by increasing (“glucose-inhibited”; GI) or decreasing (“glucose-excited”; GE) synaptic firing as ambient energy substrate levels fall (Ashford et al., 1990; Oomura et al., 1969; Silver & Erecińska, 1998). Neurotransmitter

¹School of Basic Pharmaceutical and Toxicological Sciences, College of Pharmacy, University of Louisiana Monroe, Monroe, LA, USA

Corresponding Author:

Karen P. Briski, School of Basic Pharmaceutical and Toxicological Sciences, College of Pharmacy, University of Louisiana at Monroe, 356 Bienville Building, 1800 Bienville Drive, Monroe, LA 71201, USA.
Email: briski@ulm.edu



effectors of ventromedial hypothalamic energy imbalance include γ -aminobutyric acid (GABA), which inhibits glucagon and adrenomedullary catecholamine release during hypoglycemia (Chan et al., 2006), and the gluco-stimulatory signal nitric oxide (NO), which increases counter-regulatory hormone secretion (Fioramonti et al., 2010; Routh et al., 2014). The ultra-sensitive energy gauge 5'-AMP-activated protein kinase (AMPK) is activated by phosphorylation in response to augmented cellular AMP/ATP (López, 2018; Pimentel et al., 2013; Xue & Kahn, 2006). Mediobasal hypothalamic (MBH) AMPK activation is obligatory for optimum counter-regulatory reactivity to IIIH (Han et al., 2005; McCrimmon et al., 2008). The VMN is a crucial site for integration of nutrient, endocrine, and neurochemical indicators of metabolic state that shape glucose counter-regulation; within the MBH, it is a plausible source of AMPK gluco-regulatory signaling as hypoglycemia increases AMPK phosphorylation in VMN GABAergic and nitrenergic neurons (Briski et al., 2020; Ibrabim et al., 2020).

Astrocytes support neuro-energetic stability by uptake, storage, and metabolism of glucose, the primary energy source to the brain. Glucose is processed within the astrocyte compartment to yield the oxidizable substrate fuel L-lactate (Laming et al., 2000) for transfer to neurons by cell type-specific monocarboxylate transporters (Bröer et al., 1997). Prior to entry into the astrocyte glycolytic pathway, a significant proportion of glucose is processed through the glycogen shunt, which involves successive glucose assembly into and release from this complex carbohydrate polymer (Obel et al., 2012; Schousboe et al., 2010; Shulman et al., 2001). Astrocyte glycogen mass is actively remodeled during metabolic homeostasis, and is a vital source of L-lactate equivalents during states of heightened neurological activity or glucose deficiency. Glycogen metabolism is controlled by opposing actions of the enzymes glycogen synthase (GS) and glycogen phosphorylase (GP), which respectively catalyze glycogen synthesis or glycogenolysis. Brain glycogenolysis is heightened under circumstances where energy supply is inadequate to fulfill demand, for example, seizure, sleep deprivation, and hypoglycemia (Brown, 2004; Gruetter, 2003; Schousboe et al., 2010), to liberate glucosyl units for conversion to lactate (Bélanger et al., 2011; Stobart & Anderson, 2013). Brain GP-muscle (GPmm) and -brain (GPbb) type isoforms differ with respect to cell-type localization and regulation (Nadeau et al., 2018). The astrocyte cell compartment contains GPmm and GPbb, yet the latter protein also is also expressed, albeit at lower levels, in neurons. Although phosphorylation causes complete (GPmm) or partial (GPbb) isoform activation, GPbb has a greater affinity for and sensitivity to AMP activation than GPmm and requires AMP binding for optimal enzyme function and Km. GPmm and GPbb are reported to correspondingly mediate noradrenergic or glucoprivic induction of glycogenolysis in vitro (Müller et al., 2014).

Targeted delivery of the nonselective GP inhibitor 1,4-dideoxy-1,4-imino-D-Arabinitol to the VMN increases

expression of the NO marker protein neuronal NO synthase (nNOS), and inhibits glutamate decarboxylase_{65/67} (GAD) content, findings that infer that glycogen metabolism shapes VMN gluco-regulatory signaling (Briski et al., 2021). Effects of glycogen disassembly mediated by GPmm versus GPbb during distinctive neuro-energetic states on VMN metabolic-sensory nerve cell function are unclear. Current research utilized siRNAs for GPmm or GPbb knockdown, in conjunction with combinatory immunocytochemistry/single-cell laser-catapult microdissection and high-sensitivity Western blot techniques to investigate how GP isoforms regulate VMN nitrenergic and/or GABAergic transmission and AMPK activity during glucostasis versus neuro-glucopenia. In light of recent evidence for regional variation in hypoglycemia-associated patterns of VMN GP variant expression (Uddin et al., 2020), here, target protein expression was evaluated in pure subpopulations of nitrenergic and GABAergic neurons collected at distinctive rostro-caudal levels of the VMN.

Materials and Methods

Animals: Adult female Sprague Dawley rats (220–260 gm *bw*) were group-housed in shoe-box cages (2–3 animals per cage), under a 14 h light/10 h dark cycle (lights on at 05.00 h). Animals were fed standard laboratory chow (Harlan Teklad LM-485; Harlan Industries, Madison, WI) and watered ad-libitum, and acclimated to daily handling before experimentation. All surgical and experimental protocols were carried out in accordance with the NIH Guide for Care and Use of Laboratory Animals, 8th Edition, under approval by the ULM Institutional Animal Care and Use Committee.

Experimental Design: Animals were randomly assigned to one of six treatment groups ($n = 4/\text{group}$). On day 1, rats were bilaterally ovariectomized and implanted subcutaneously (*sc*) with a 17 β estradiol-3-benzoate—filled silastic capsule (30 $\mu\text{g}/\text{mL}$ safflower oil; *i.d.* 0.062/in., *o.d.* 0.125 in.; 10 mm/100 g *bw*), under ketamine/xylazine (0.1 mL/100 g *bw*; 90 mg ketamine, 10 mg xylazine/mL; Henry Schein, Inc., Melville, NY) anesthesia. This steroid replacement regimen yields approximate plasma estradiol concentrations of 22 pg/mL (Briski et al., 2001) to replicate circulating hormone levels characteristic of metestrus in a 4-day cycle (Butcher et al., 1974). Rats were bilaterally injected into the VMN with Accell™ controlled nontargeting pool (scramble; SCR) siRNA (500 pmol; prod. no.: D-001910-10-20; Dharmacon Inc., Lafayette, CO; groups 1 and 4); Accell™ rat PYGB siRNA (500 pmol, Suzuki et al., 2010; prod. no.: EQ-093001-00-05; gene id-25739; Dharmacon; groups 2 and 5), or Accell™ rat PYGM siRNA (500 pmol, Suzuki et al., 2010); prod. no.: EQ-101552-00-05; gene ID-24701; groups 3 and 6), by stereotaxic drill and injection robot (Neurostar, Tubingen, Germany), at preset three-dimensional coordinates (2.50 mm posterior to *bregma*; 0.6 mm lateral to

midline; 9.0 mm below skull surface). After surgery, rats were injected with ketoprofen (1 mg/kg *bw*, *sc*; Zoetis, MI) and enrofloxacin (IM; 10 mg/0.1 mL; Bayer HealthCare LLC, Germany), treated by topical administration of 0.25% bupivacaine (Hospira, Inc., IL) to the suture site, and transferred to individual cages. At 09.00 h on day 7, rats were injected *sc* with sterile INS diluent (V; Eli Lilly and Company, Indianapolis, IN; groups 1, 3, and 5) or neutral protamine Hagedorn INS (INS; 10 U/kg *bw*, Napit et al., 2019; groups 2, 4, and 6). Animals were sacrificed at 10.00 h on that same day for brain tissue and trunk blood collection. Plasma glucose levels were measured using an ACCU-CHECK Aviva plus glucometer (Roche Diagnostic Corporation, Indianapolis, IN) and glucagon and corticosterone concentrations were analyzed by ELISA, as described by Napit et al., 2019. Brains were snap-frozen in liquid nitrogen-cooled isopentane and stored at -80°C ; plasma was stored at -20°C .

VMN Micropunch Dissection: For each animal, the VMN was divided into rostral (-1.8 to -2.3 mm), middle (-2.3 to -2.8 mm), and caudal (-2.8 to -3.3 mm) segments. Each segment was cut into $2 \times 100 \mu\text{m}$ and $30 \times 10 \mu\text{m}$ coronal sections for microneedle punch dissection or laser-catapult microdissection, respectively. Consecutive sections were cut from each brain beginning rostral to the retrochiasmatic area, at the approximate level of the optic chiasm, until the VMN was reached; sections then cut through successive rostro-caudal VMN segments were processed for Western blot analysis of VMN tissue GP variant content (micropunch tissue samples) or neurotransmitter marker and total/phosphorylated AMPK protein expression (pure nerve cell samples acquired by *in situ* immunocytochemistry/laser-catapult microdissection). Several distinctive neuro-topographic features were used to verify the rostro-caudal progression of tissue sectioning, including continuity of the third ventricle with lateral ventricles, which occurs at the level of the suprachiasmatic nucleus; derivation of the lateral optic tracts from the midline optic chiasm; and rostro-caudal changes in the curvature of the ventral surface of the hypothalamus. Within each segment, bilateral microneedle punches of VMN tissue were taken from $100 \mu\text{m}$ -thick sections using a calibrated 0.5 mm hollow punch tool (prod. no. 57401; Stoelting Co., Kiel, WI), and pooled in lysis buffer (2.0% sodium dodecyl sulfate, 0.05 M dithiothreitol, 10.0% glycerol, 1.0 mM EDTA Ibrahim et al., 2019). Accuracy of use of micropunch technology for collection of distinctive hypothalamic loci of interest, including the VMN, as indicated by distinctive marker protein expression, has been validated (Mandal et al., 2017, 2018). For each treatment group, micropunch tissue lysate aliquots from individual subjects were combined to generate quadruplicate sample pools for each target protein, for example, GPbb and GPmm, for each rostro-caudal segment. Bilateral micropunch tissue samples were obtained from additional hypothalamic structures implicated in glucoregulation, for example, hypothalamic paraventricular (-0.7 to -2.3 mm),

dorsomedial (-2.0 to -3.8 mm), and arcuate (-1.8 to -3.2 mm) nuclei and lateral hypothalamic area (-2.3 to -3.8 mm), to determine if PYGM or PYGB siRNA delivery to the VMN altered gene product expression in those structures.

VMN GABAergic and Nitrergic Neuron Laser-Catapult Microdissection: For each rat, $10 \mu\text{m}$ -thick sections were mounted on polyethylene naphthalate membrane-coated glass slides (Carl Zeiss Microscopy LLC, White Plains NY) for storage at -20°C . Tissues were processed by peroxidase immunocytochemistry to label GAD- or nNOS-immunoreactive (-ir) neurons (Uddin et al., 2019; Ibrahim et al., 2019). Sections were fixed with acetone (5 min), then blocked (30 min) with 1.5% normal goat serum (prod. no. S-1000; Vector Laboratories, Burlingame, CA) in Tris-buffered saline, 10 mM, pH 7.4 (TBS; Sigma Aldrich, St. Louis, MO) containing 0.05% Triton X-100 prior to incubation with rabbit primary antibodies against GAD (prod. no. ABN904, 1:1000; MilliporeSigma, Burlington, MA) or nNOS (prod. no. NBPI-39681, 1:1000; Novus Biologicals, LLC, Littleton, CO) for 36–48 h at 4°C . After exposure (2 h) to horseradish peroxidase-labeled goat anti-rabbit secondary antibodies (prod. no. PI-1000, 1:1000; Vector Lab.), tissues were incubated with Vector ImmPACT diaminobenzidine substrate kit reagents (prod. no. SK-4105; Vector Laboratories). After immunocytochemical staining, VMN was differentiated from neighboring elements on the basis of its unique oblong shape and oblique orientation within the MBH, and its location relative to the arcuate nucleus, which lies ventromedial to the VMN, and optic tracts, which reside beneath the lateral zone of the lateral hypothalamic area. VMN GAD- or nNOS-ir neurons were laser-catapult microdissected from immunolabeled sections (Figure 1). Distinctive neuroanatomical features, such as rostro-caudal changes in morphological features of the arcuate nucleus (which exhibits a “horse-shoe” shape as its far rostral part is located directly beneath the third ventricle, but gives rise more caudally to bilateral elements situated on either side of the third ventricle) and conformation changes in the median eminence (which transforms from a horizontal structure located beneath the third ventricle into the infundibulum, which detaches from the ventral surface of the brain) were utilized to verify accurate identification of the VMN. Within each rostro-caudal VMN segment, individual GAD- or nNOS-ir neurons were harvested with a Zeiss P.A.L.M. UV-A microlaser IV. Previous Western blot analysis showed that the anti-GAD and -nNOS primary antisera used here each detect a single protein band of expected antigen molecular weight in lysates of micropunched VMN tissue (Uddin et al., 2020). Figure 1 contains whole immunoblots that verify the specificity of GAD or nNOS protein detection in pure VMN nerve cell lysates. Within each treatment group, nitrergic or GABAergic lysate aliquots from individual subjects were combined to create quadruplicate sample pools ($n=50$ cells per group) for each protein of interest within each VMN segment.

Western Blot Analysis: Proteins were electrophoresed in Bio-Rad TGX 10% stain-free gels (prod. no. 161-0183,

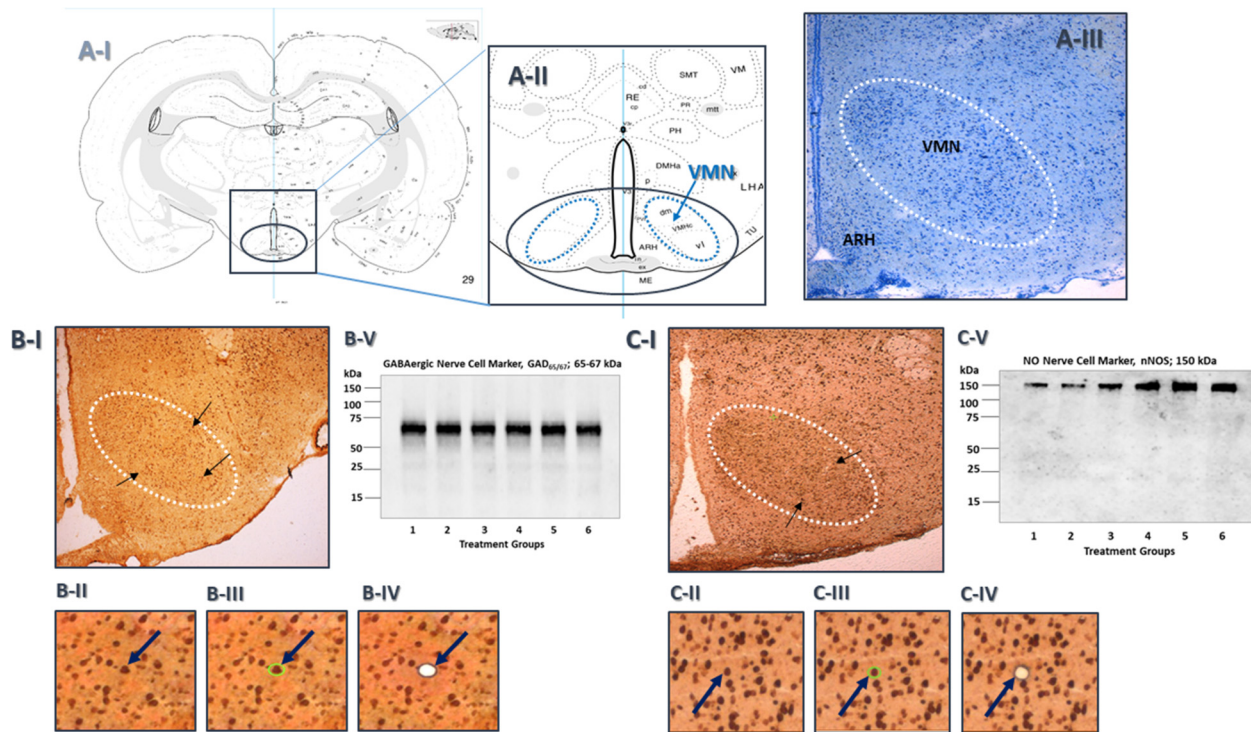


Figure 1. Laser-Catapult microdissection of immunolabeled VMN NO or GABA neurons. Rat brain coronal brain sections illustrated in Panels A-I and A-II depict the orientation of the VMN (bilateral oblong ovals; dotted blue lines) within the mediobasal hypothalamus (midline oval; solid blue line). The methylene blue-stained tissue section in Panel A-III shows the demarcation of the VMN (white dotted-line oval) from surrounding structures, including the ARH. Characteristic distribution pattern of GAD-ir-positive neuron perikarya (indicated by blue arrows) within the VMN is shown in Panel B-I. The area depicted in Panel B-II featuring a GAD-ir neuron (blue arrow) was re-photographed after positioning of a continuous laser track (depicted in green) [Panel B-III] and subsequent ejection of that neuron by laser pulse [Panel B-IV]. The whole immunoblot in Panel B-V shows that the GAD primary antiserum detected a single band of antigen of predicted molecule weight in VMN GAD-ir nerve cell lysates from treatment groups 1–6, defined in the Materials and Methods section. Images in Panels C-I–C-IV illustrate a representative pattern of nNOS immunostaining of the VMN, and laser-assisted collection of a single nNOS-ir neuron (blue arrow) from a tissue section cut through that structure. The whole blot in Panel C-V indicates selective detection of nNOS protein in VMN nNOS-ir neuronal lysates from each treatment group. Note that this microdissection technique causes negligible destruction of surrounding tissue and minimal inclusion of adjacent tissue.

Abbreviations: VMN = ventromedial hypothalamic nucleus; NO = nitric oxide; GABA = γ -aminobutyric acid; ARH = arcuate hypothalamic nucleus; GAD = glutamate decarboxylase_{65/67}; nNOS = neuronal nitric oxide synthase.

Bio-Rad Laboratories Inc., Hercules CA Hercules, CA). Prior to trans-blotting to 0.45- μ m PVDF-Plus membranes (prod. no. 1212639; Data Support Co., Panorama City, CA), gels were UV light-activated (1 min) in a BioRad ChemiDoc TM Touch Imaging System (Hercules, CA) (Ibrahim et al., 2019). Membranes were blocked with TBS containing 0.1% Tween-20 (Amresco LLC, Solon, OH) and 2.0% bovine serum albumin (MP Biomedicals LLC, Santa Ana, CA), then incubated (36–42 h; 4°C) with rabbit primary polyclonal antisera against GPbb (1:2,000; prod. no. NBP1-32799; Novus Biologicals, Littleton, CO), GPmm (1:2,000; prod. no. NBP2-16689; Novus Biol.), GAD (1:10,000; prod. no. ABN904; Millipore Sigma, Burlington, MA), nNOS (1:1,500; prod. no. NBP1-39681; Novus Biol.), AMPK $\alpha_{1,2}$ (prod. no. 2532S, 1:2,000; Cell Signaling Technology Inc., Danvers, MA), or phosphoAMPK $\alpha_{1/2}$ (Thr 172) (pAMPK; prod. no. 2535S, 1:2,000; Cell Signaling Technol.). Membranes were

next incubated with (4 h; 4°C) goat anti-rabbit secondary antibodies (1:5,000; prod. no. NEF812001EA; PerkinElmer, Waltham, MA), followed by SuperSignal West Femto maximum sensitivity chemiluminescent substrate (prod. no. 34096; Thermo Fisher Scientific, Rockford, IL). Membrane blocking, buffer washes, and antibody incubations were performed by automation in a Freedom Rocker Blotbot (Next Advance, Inc., Troy, NY). Chemiluminescence optical density (OD) values were normalized to total in-lane protein using BioRad Image Lab™ 6.0.0 software. Precision plus protein molecular weight dual-color standards (prod. no. 161-0374, BioRad) were included in each Western blot analysis.

Statistical Analyses: Mean normalized VMN rostro-caudal segment-specific micropunch or nerve cell protein O.D. and plasma glucose and hormone data were evaluated by two-way analysis of variance and Student–Newman–Keuls post-hoc test. Differences of $p < .05$ were considered

significant. In each figure, statistical differences between specific pairs of treatment groups are denoted as follows: * $p < .05$; ** $p < .01$; *** $p < .001$; **** $p < .0001$.

Results

Data shown in Figure 2 illustrate effects of bilateral SCR versus GP isoform siRNA administration to the VMN on GPbb and GPmm protein expression over the rostro-caudal length of this nucleus. GPbb knockdown significantly reduced GPbb protein content of micropunch-dissected tissue collected from rostral (Figure 2A) [$F_{(5,18)} = 16.78$; $p < .0001$], middle (Figure 2C) [$F_{(5,18)} = 84.96$; $p < .0001$], or caudal (Figure 2E) [$F_{(5,18)} = 17.63$; $p < .0001$] levels of the VMN (GPbb siRNA/V [diagonal-striped white bar] vs. SCR/V [solid white bar]). GPbb siRNA attenuated hypoglycemia-associated up-regulation of GPbb expression in each VMN segment versus SCR pretreatment (GPbb siRNA/INS [diagonal-striped gray bar] vs. SCR siRNA/INS [solid gray bar]). Data also show that animals given GPbb

siRNA showed significant diminution of middle VMN GPmm protein expression, yet enhanced middle and caudal GPmm content after INS injection. GPmm siRNA down-regulated GPmm protein profiles in the rostral (Figure 2B) [$F_{(5,18)} = 34.85$; $p < .0001$], middle (Figure 2D) [$F_{(5,18)} = 19.57$; $p < .0001$], and caudal (Figure 2F) [$F_{(5,18)} = 21.16$; $p < .0001$] VMN (GPmm siRNA/V [cross-hatched white bar] vs. SCR/V [solid white bar]). GPmm knockdown suppressed VMN GPmm protein expression after INS injection versus SCR-pretreated rats (GPmm siRNA/INS [cross-hatched gray bar] vs. SCR siRNA/INS [solid gray bar]).

Figure 3 depicts the effects of intra-VMN GPbb or GPmm siRNA administration on VMN nitric oxide synthase (nNOS) protein expression in V- or INS-injected rats. Baseline nNOS levels in NO neurons collected from the rostral (Figure 3A) [$F_{(5,18)} = 12.68$; $p < .0001$], middle (Figure 3B) [$F_{(5,18)} = 33.11$; $p < .0001$], or caudal (Figure 3C) [$F_{(5,18)} = 11.39$; $p < .0001$] VMN were not different between SCR versus GP siRNA-pretreated groups. INS injection significantly increased nNOS content in cells taken from each

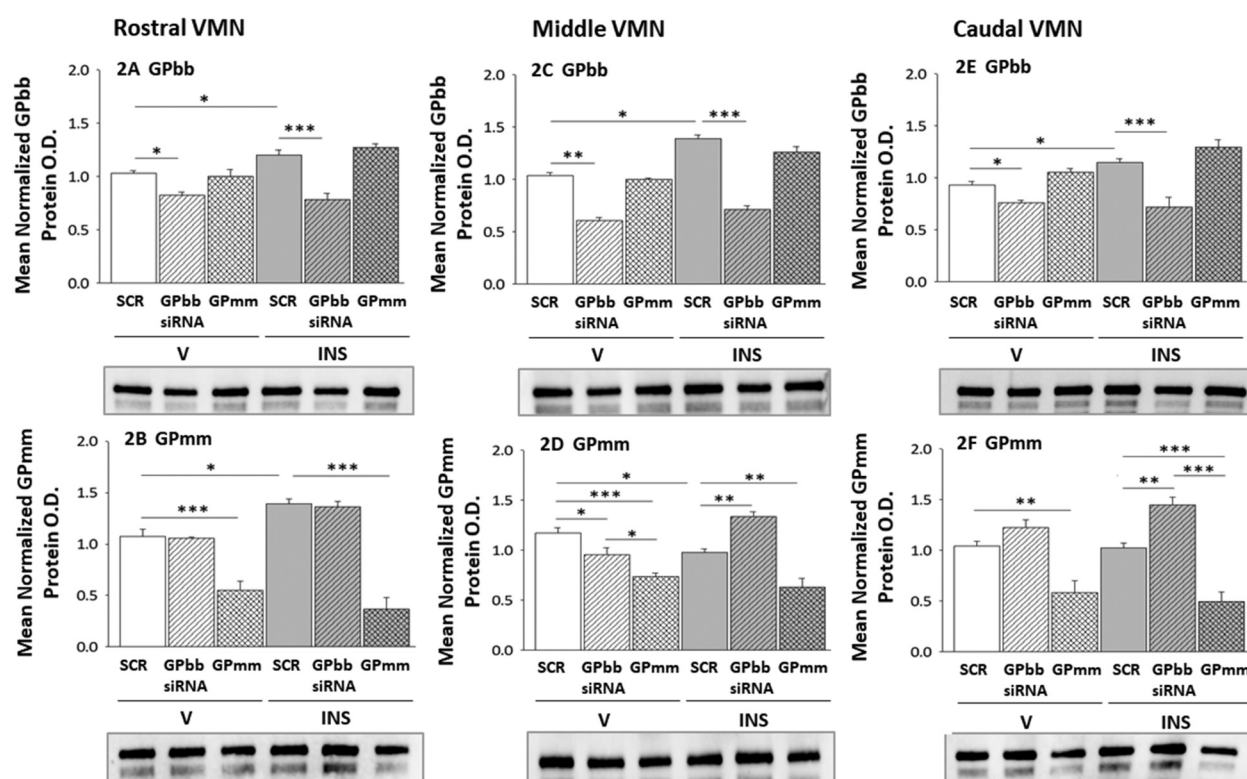


Figure 2. Effects of intra-VMN administration of SCR versus GPbb or GPmm siRNA on VMN GPbb and GPmm protein expression. VMN tissue was bilaterally micropunch-dissected from rostral (left-hand column), middle (middle column), and caudal (right-hand column) VMN fresh-frozen tissue sections after sc V or INS injection into SCR-, GPbb, or GPmm-siRNA-pretreated animals. Data show mean normalized GPbb (A, C, E) or GPmm (B, D, F) protein OD measures \pm SEM for the following treatment groups ($n = 4$ per group): SCR/V (solid white bars), GPbb siRNA/V (diagonal-striped white bars), GPmm siRNA/V (cross-hatched white bars), SCR/INS (solid gray bars), GPbb siRNA/INS (diagonal-striped gray bars), and GPmm siRNA/INS (cross-hatched gray bars). * $p < .05$; ** $p < .01$; *** $p < .001$.

Abbreviations: VMN = ventromedial hypothalamic nucleus; SCR = scramble; GP = glycogen phosphorylase; GPbb = glycogen phosphorylase-brain type; GPmm = glycogen phosphorylase-muscle type; OD = optical density; SEM = standard error of mean; INS = insulin; V = vehicle; sc = subcutaneous.

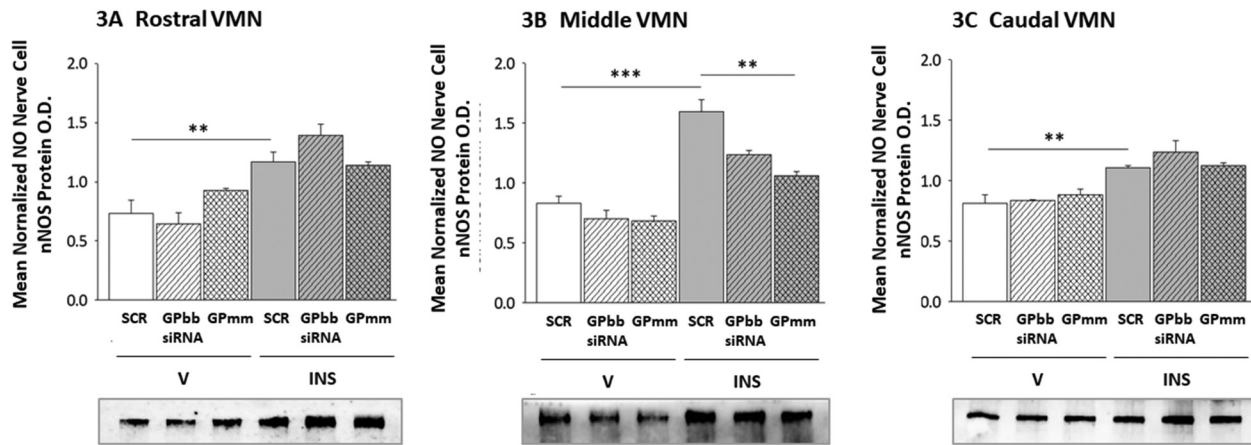


Figure 3. Effects of GP isoform knockdown on VMN NO nerve cell transmitter marker expression. For each animal, nNOS-immunopositive neurons were collected by laser-catapult microdissection and pooled separately within rostral (left-hand column), middle (middle column), and caudal (right-hand column) VMN segments. Data depict mean normalized nNOS protein OD measures \pm SEM for rostral (A), middle (B), and caudal (C) VMN NO neurons from SCR/V (solid white bars), GPbb siRNA/V (diagonal-striped white bars), GPmm siRNA/V (cross-hatched white bars), SCR/INS (solid gray bars), GPbb siRNA/INS (diagonal-striped gray bars), and GPmm siRNA/INS (cross-hatched gray bars) treatment groups. * $p < .05$; ** $p < .01$; *** $p < .001$. Abbreviations: GP = glycogen phosphorylase; VMN = ventromedial hypothalamic nucleus; NO = nitric oxide; nNOS = neuronal nitric oxide synthase; OD = optical density; SEM = standard error of measurement; INS = insulin; SCR = scramble.

region. Hypoglycemic up-regulation of this protein was reversed by GPmm siRNA. Data in Figure 4 show that rostral (Figure 4A) [$F_{(5,18)} = 10.45$; $p < .0001$], middle (Figure 4B) [$F_{(5,18)} = 13.56$; $p < .0001$], and caudal (Figure 4C) [$F_{(5,18)} = 7.89$; $p < .0001$] VMN nitrenergic nerve cell total AMPK profiles were diminished by GPmm knockdown. AMPK expression in caudal VMN NO neurons was also suppressed by GPbb siRNA. Hypoglycemia significantly inhibited this protein in nitrenergic neurons located throughout the VMN. In the rostral and caudal VMN, this inhibitory response was averted by GPmm knockdown. Figure 4 also depicts the effects of siRNA pretreatment on the expression of the activated, for example, phosphorylated form of AMPK. Data in Figure 4B, D and F show that baseline NO nerve cell pAMPK expression is refractory to GP variant control. Hypoglycemia-associated up-regulation of this protein was attenuated (rostral VMN; Figure 4B) [$F_{(5,18)} = 29.80$; $p < .0001$] or exacerbated (caudal VMN; Figure 4F) [$F_{(5,18)} = 12.18$; $p < .0001$] by GPbb, according to VMN segment. Meanwhile, GPmm knockdown amplified hypoglycemic stimulation of middle VMN nitrenergic cell pAMPK expression (Figure 4D) [$F_{(5,18)} = 13.97$; $p < .0001$].

Effects of SCR versus GP siRNA on VMN GABAergic neuron GAD protein expression are shown in Figure 5. GPbb or GPmm knockdown inhibited GAD expression in caudal (Figure 5C) [$F_{(5,18)} = 10.38$; $p < .0001$], but not rostral (Figure 5A) [$F_{(5,18)} = 10.83$; $p < .0001$] or middle (Figure 5B) [$F_{(5,18)} = 22.35$; $p < .0001$] VMN GABA cells. GPbb siRNA attenuated (rostral VMN) or intensified (middle and caudal VMN) hypoglycemia-associated down-regulation of GAD, in a segment-specific manner. Figure 6 illustrates the effects of GPbb or GPmm knockdown on

GABAergic nerve cell AMPK and pAMPK expression. GABA cell AMPK content was suppressed in the rostral VMN by GPbb or GPmm siRNA (Figure 6A) [$F_{(5,18)} = 11.23$; $p < .0001$], but was diminished by GPmm or GPbb knockdown in middle (Figure 6C) [$F_{(5,18)} = 32.92$; $p < .0001$] or caudal (Figure 6E) [$F_{(5,18)} = 9.57$; $p < .0001$] segments, respectively. In the middle VMN, hypoglycemic inhibition of this protein profile was reversed by GPmm siRNA, whereas GPbb knockdown suppresses AMPK levels in caudal VMN GABA neurons. Figure 6B shows that the rostral VMN GABAergic neuron exhibit up-regulated pAMPK levels following GPbb or GPmm siRNA administration [$F_{(5,18)} = 10.72$; $p < .0001$]. GPbb knockdown also increased pAMPK expression in caudal VMN GABA cells (Figure 6F) [$F_{(5,18)} = 10.49$; $p < .0001$]. Hypoglycemia up-regulated pAMPK expression in GABA nerve cells from the middle (Figure 6D) [$F_{(5,18)} = 13.27$; $p < .0001$] and caudal VMN. In both segments, this stimulatory effect was augmented by GPbb knockdown.

Figure 7 depicts the patterns of GP isoform protein profiles in the PVN (Figure 7A), DMN (Figure 7B), LHA (Figure 7C), and ARH (Figure 7D) after intra-VMN GP siRNA administration. Data show that neither GPbb nor GPmm siRNA delivery to the VMN altered gene product expression in the PVN (GPbb, at right [$F_{(2,6)} = 1.63$; $p = .245$]; GPmm, at left [$F_{(2,6)} = 3.32$; $p = .083$]), DMN (GPbb, at right [$F_{(2,6)} = 3.895$; $p = .060$]; GPmm, at left [$F_{(2,6)} = 3.169$; $p = .091$]), LHA (GPbb, at right [$F_{(2,6)} = 0.97$; $p = .415$]; GPmm, at left [$F_{(2,6)} = 3.98$; $p = .058$]), or ARH (GPbb, at right [$F_{(2,6)} = 1.24$; $p = .353$]; GPmm, at left [$F_{(2,6)} = 1.69$; $p = .260$]).

Data in Figure 8 illustrate the effects of intra-VMN SCR, GPbb, or GPmm siRNA administration on circulating

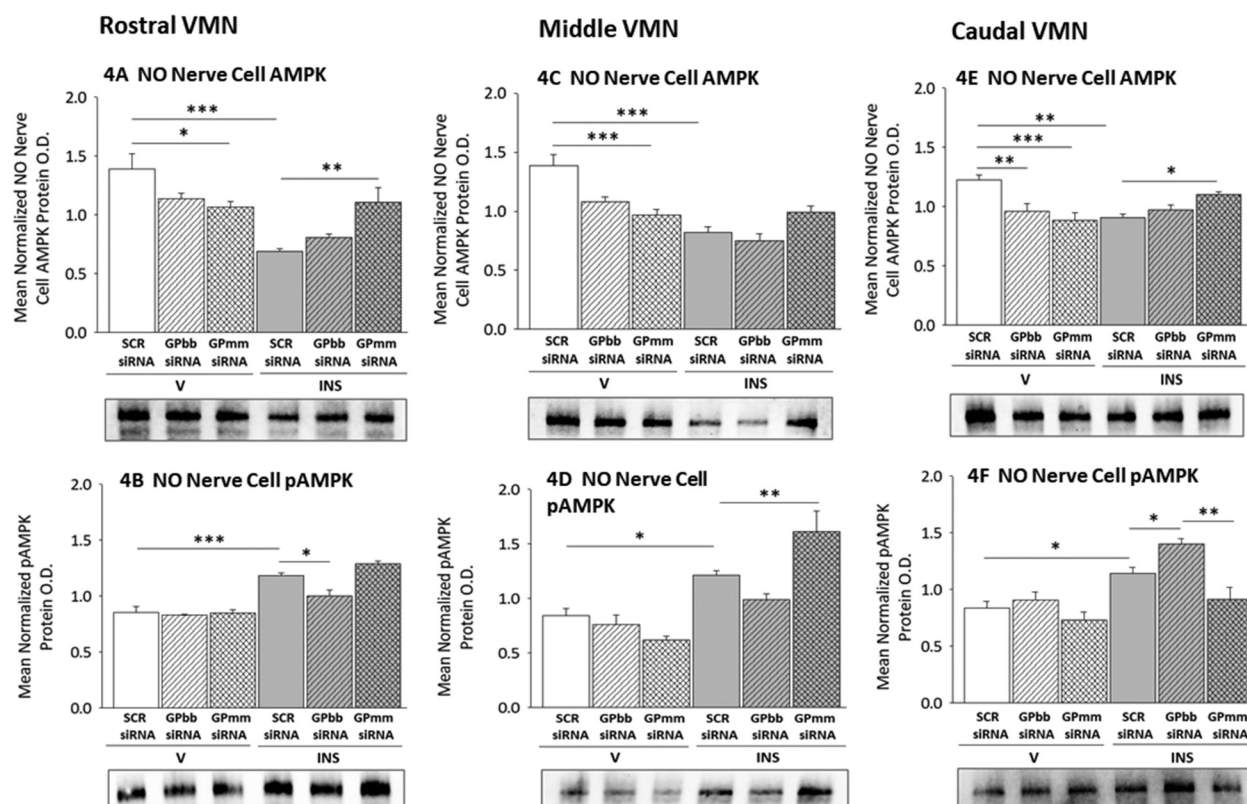


Figure 4. GPbb versus GPmm regulation of VMN NO neuron total and phosphorylated AMPK protein expression. Western blot analysis of rostral (left-hand column), middle (middle column), and caudal (right-hand column) VMN NO neurons was performed to determine effects of GP isoform knockdown on total AMPK and pAMPK protein expression during glucostasis versus glucoprivation. For each VMN segment, data show mean normalized AMPK (A, C, E) or pAMPK (B, D, F) protein OD measures \pm SEM for NO neurons collected from SCR-, GPbb-, or GPmm siRNA-pretreated animals after sc injection of V or INS. * $p < .05$; ** $p < .01$; *** $p < .001$.

Abbreviations: GPbb = glycogen phosphorylase-brain type; GPmm = glycogen phosphorylase-muscle type; VMN = ventromedial hypothalamic nucleus; NO = nitric oxide; AMPK = 5'-AMP-activated protein kinase; OD = optical density; SEM = standard error of mean; pAMPK = phosphorylated AMPK; SCR = scramble; INS = insulin; V = vehicle; sc = subcutaneous.

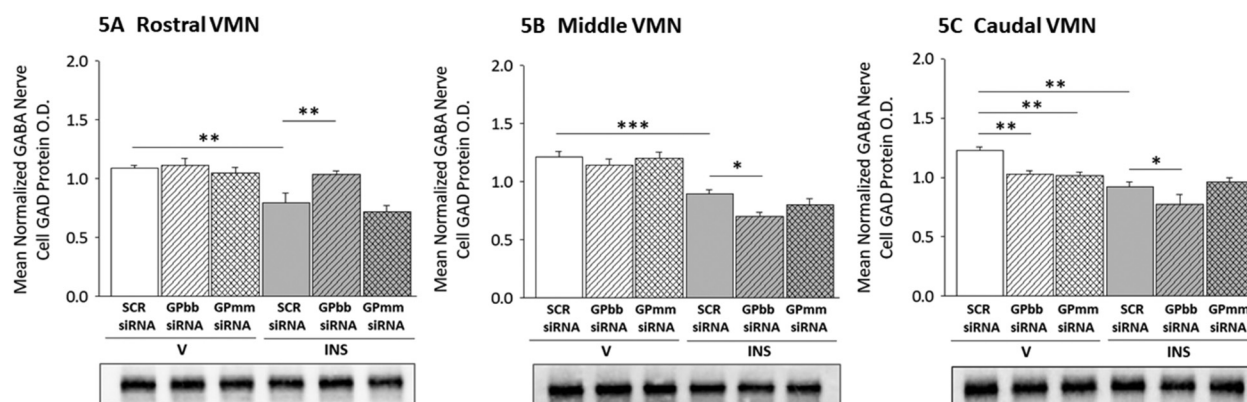


Figure 5. Effects of GP isoform knockdown on VMN GABA neuron GAD protein expression. Data depict mean normalized GAD protein OD values \pm SEM for GAD-immunolabeled neurons harvested from rostral (A), middle (B), and caudal (C) VMN segments of SCR/V (solid white bars), GPbb siRNA/V (diagonal-striped white bars), GPmm siRNA/V (cross-hatched white bars), SCR/INS (solid gray bars), GPbb siRNA/INS (diagonal-striped gray bars), and GPmm siRNA/INS (cross-hatched gray bars) treatment groups. * $p < .05$; ** $p < .01$; *** $p < .001$. Abbreviations: GP = glycogen phosphorylase; VMN = ventromedial hypothalamic nucleus; GABA = γ -aminobutyric acid; GAD = glutamate decarboxylase_{65/67}; OD = optical density; SEM = standard error of mean; SCR = scramble; INS = insulin; V = vehicle; sc = subcutaneous.

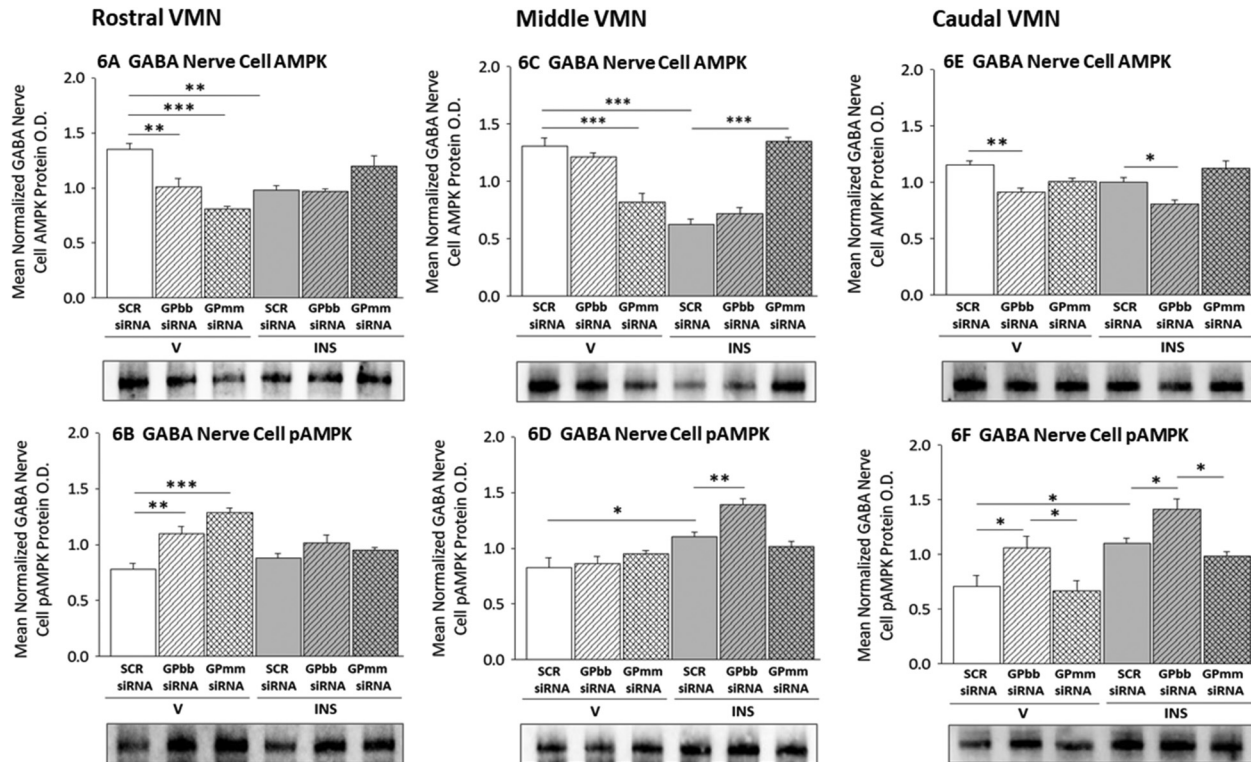


Figure 6. GPbb versus GPmm regulation of VMN GABA neuron total and phosphorylated AMPK protein expression. Western blot analysis of rostral (left-hand column), middle (middle column), and caudal (right-hand column) VMN GABA neurons was performed to determine effects of GP isoform knockdown on total AMPK and pAMPK protein expression during glucostasis versus glucoprivation. For each VMN segment, data show mean normalized AMPK (A, C, E) or pAMPK (B, D, F) protein OD measures \pm SEM for GAD-immunopositive neurons collected from SCR-, GPbb-, or GPmm siRNA-pretreated animals after sc injection of V or INS. * $p < .05$; ** $p < .01$; *** $p < .001$.

Abbreviations: GPbb = glycogen phosphorylase-brain type; GPmm = glycogen phosphorylase-muscle type; VMN = ventromedial hypothalamic nucleus; GABA = γ -aminobutyric acid; NO = nitric oxide; AMPK = 5'-AMP-activated protein kinase; OD = optical density; SEM = standard error of mean; pAMPK = phosphorylated AMPK; GAD = glutamate decarboxylase_{65/67}; SCR = scramble; INS = insulin; V = vehicle; sc = subcutaneous.

glucose (Figure 8A [$F_{(5,18)} = 10.38$; $p < .0001$]), glucagon (Figure 8B [$F_{(5,18)} = 12.98$; $p < .0001$]), and corticosterone (Figure 8C [$F_{(5,18)} = 34.73$; $p < .0001$]) levels after sc V or INS injection. Plasma glucose values measured after V injection were similar among groups despite different pretreatments. Glucose decrements due to INS did not differ between SCR versus GP siRNA pretreated rats. Basal glucagon secretion was unaffected by either GP siRNA, whereas GPbb or GPmm knockdown caused statistically nonsignificant attenuation of hypoglycemic augmentation of glucagon release. Animals pretreated with GPbb siRNA administration exhibited significantly higher plasma corticosterone levels after V or INS injection compared to SCR administration.

Discussion

The VMN integrates diverse metabolic cues, including glycogen metabolic status to shape neural control of counter-regulation. Norepinephrine-sensitive GPmm and AMP-sensitive GPbb isoforms confer stimulus-specific regulation of brain glycogen.

Current research extends prior work involving nonselective pharmacological inhibition of VMN GP by use here of gene silencing tools to investigate the distinctive roles of GPmm versus GPbb in VMN gluco-regulatory signaling during eu- and hypoglycemia. Outcomes provide novel proof that GPbb regulates hypoglycemic patterns of GPmm expression. Data show that within defined rostro-caudal segments of the VMN, glycogenolysis mediated by either GP variant controls homeostatic patterns of GABAergic transmission whereas GABA and NO signal responses to hypoglycemia reflect, in part, glycogen breakdown involving GPbb or -mm, respectively. Both GP isoforms regulate GABA and NO nerve cell AMPK protein profiles during euglycemia, but GPmm-controlled glycogen disassembly mediates hypoglycemic suppression of AMPK in each neuron type. Conversely, GPbb-regulated glycogenolysis exerts segment-specific bi-directional effects on hypoglycemic up-regulation of pAMPK in nitroergic neurons, but attenuates activation of this sensor in GABA cells. Amplification of hypoglycemic augmentation of metabolic-sensory nerve cell pAMPK by GPbb knockdown infers that glycogen mobilization by

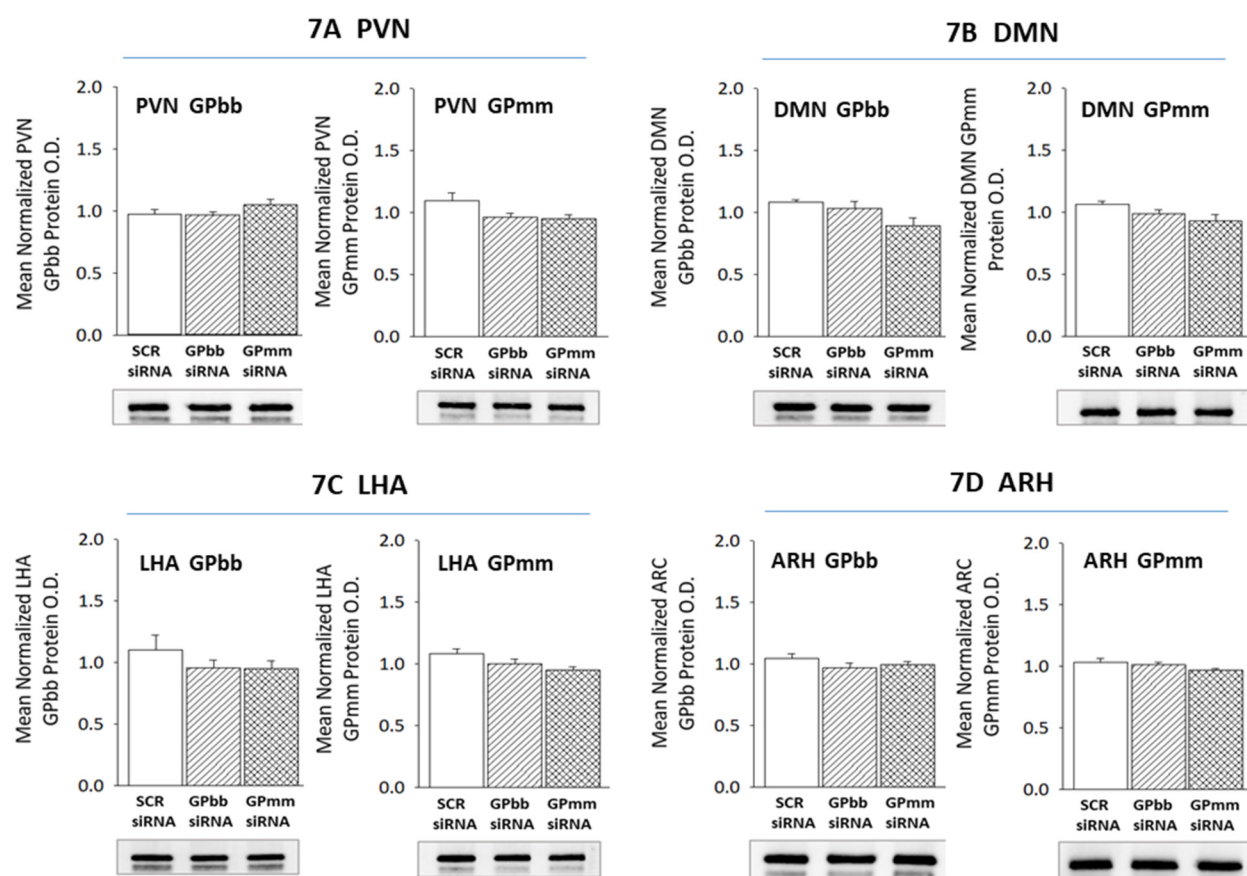


Figure 7. Effects of intra-VMN GP siRNA administration on PVN, DMN, and ARH hypothalamic nucleus and LHA GP variant protein expression. Data show mean normalized GPbb (at right) or GPmm (at left) PVN (A), DMN (B), LHA (C), and ARH (D) protein OD values \pm SEM after administration of SCR, GPbb siRNA, or GPmm siRNA to the VMN.

Abbreviations: VMN = ventromedial hypothalamic nucleus; GP = glycogen phosphorylase; PVN = paraventricular; DMN = dorsomedial; ARH = arcuate; LHA = lateral hypothalamic area; GPbb = glycogen phosphorylase-brain type; GPmm = glycogen phosphorylase-muscle type; OD = optical density; SEM = standard error of mean; SCR = scramble.

this GP isoform lessens neuronal energy instability during neuro-glucopenia. Evidence for GPbb siRNA up-regulation of hypoglycemic hypercorticotestosterone implicates VMN GPbb-mediated glycogenolysis in neural regulation of this counter-regulatory response.

Outcomes validate the utility of stereotaxic GP siRNA administration for structure-specific isoform knockdown *in vivo*. Alongside suppression of VMN GPbb protein content, GPbb siRNA treatment down-regulated basal GPmm profiles, yet amplified expression of GPmm during hypoglycemia in discrete rostro-caudal VMN segments. It is speculated that diminished GPbb-mediated glycogenolysis during energy homeostasis may be construed as an indicator of glycogen depletion, which might in turn impede GPmm disassembly of glycogen in order to conserve glycogen mass. Similarly, amplification of hypoglycemic up-regulation of GPmm profiles by GPbb knockdown may reflect a switch in stimulus-specific glycogen breakdown triggered by diminution of glycogen mass capable of disassembly by the AMP-sensitive GP isoform. Additional research is needed

to ascertain the ratio of GPbb versus GPmm protein expression in VMN astrocytes under conditions of glucose sufficiency versus deficiency. There is also a need to determine if astrocyte glycogen in its entirety is a common substrate for GPbb versus GPmm breakdown, or alternatively, if this fuel reserve is organized into spatially distinct pools that are disassembled by a single GP variant. It should be noted that siRNA-mediated adjustments in total GPbb or GPmm protein expression do not provide definitive evidence for coincident change in isoform enzyme activity, as analytical tools for quantification of GP variant phosphorylation *in vivo* are not unavailable.

Current data show that neither GP siRNA altered nNOS content of VMN nitroergic neurons obtained under euglycemic conditions, which infers that glycogen disassembly may not significantly affect baseline gluco-stimulatory NO transmission. Hypoglycemia up-regulated NO nerve cell nNOS expression in all rostro-caudal VMN segments; however, this stimulatory response was blunted by GPmm knockdown in the middle VMN, which suggest that decreased

GPmm-mediated glycogen mobilization represses NO signal input to local gluco-regulatory circuitries. The mechanisms that underlie VMN segment-specific GPmm knockdown effects on this transmitter marker protein during hypoglycemia remain unclear. Nitroergic nerve cell total AMPK protein content was down-regulated by GPmm siRNA throughout the length of the VMN, as well as by GPbb knockdown in the caudal VMN. Interestingly, GPmm knockdown reversed hypoglycemic down-regulation of AMPK in NO cells collected from rostral and caudal VMN segments. In those locations, GPmm-mediated glycogen breakdown may thus serve as a positive stimulus for nitroergic neuron AMPK expression during euglycemia, yet may be inhibitory to this protein profile during hypoglycemia. The sequelae of GPmm action on astrocyte glycogen that control NO cell AMPK protein expression remain to be identified. It would be informative to learn how reductions in GPmm-controlled glycogenolysis exert opposite regulatory effects on this protein profile during glucostasis versus glucoprivation. Neither GP siRNA altered pAMPK protein content of nitroergic neurons from euglycemic rats, inferring that the energy status of these cells is unaffected by glycogen metabolism during energy homeostasis. Evidence here for coincident hypoglycemic up-regulation of pAMPK and nNOS profiles suggests that elevated gluco-stimulatory signaling by VMN nitroergic neurons reflects their state of metabolic imbalance. GPbb siRNA attenuated (rostral VMN) or augmented (caudal VMN) this pAMPK up-regulation; hypoglycemic patterns of GPbb-mediated glycogenolysis may thus correspondingly drive or blunt NO nerve cell AMPK activation in those sites. On the other hand, GPmm knockdown amplified hypoglycemic stimulation of NO neuron pAMPK profiles in mid-level of the VMN. These results show that during hypoglycemia, glycogen regulation of VMN nitroergic neuron energy stability is GP isoform-specific within each rostro-caudal region, and that GPbb-mediated glycogenolysis has a relatively broader impact on NO nerve cell AMPK activity during neuro-glucopenia. Observations here that GPmm siRNA treatment likely attenuates hypoglycemic patterns of NO release despite having an amplifying effect on pAMPK expression imply that GPmm may regulate this transmitter by a mechanism(s) unrelated to AMPK.

In GABA neurons acquired from euglycemic rats, the transmitter marker protein GAD was down-regulated by GP knockdown in the caudal, but not rostral or middle VMN; thus, in that distinct location, glycogen turnover may stimulate gluco-inhibitory GABAergic transmission during energy homeostasis. Data show that hypoglycemia-associated down-regulation of GABA nerve cell GAD profiles was reversed (rostral VMN) or exacerbated (middle and caudal VMN) by GPbb siRNA treatment. Thus, in the rostral VMN, GPbb-controlled glycogenolysis may mediate hypoglycemia-associated inhibition of this neurotransmitter, whereas, in other VMN segments, GPbb may restrain the negative GAD response to hypoglycemia. Suppressive effects of GP knockdown on GABA nerve cell AMPK protein expression infer that glycogen turnover stimulates this protein profile

throughout the VMN. Hypoglycemia reduced AMPK levels in rostral and middle VMN GABAergic neurons. Reversal of this inhibitory response by GPmm knockdown implicates GPmm in this regulatory action. Results show that GABA nerve cell pAMPK levels were increased in a segment-specific manner by GPbb (rostral and caudal VMN) or GPmm (rostral VMN) knockdown respectively, implying that in those sites glycogen metabolism enhances metabolic stability of these neurons. Evidence for amplification of hypoglycemia-associated up-regulation of GABA neuron pAMPK content by GPbb knockdown infers that glycogenolysis controlled by this GP variant mitigates metabolic instability in these cells during neuro-glucopenia. Observations of parallel intensification of middle and caudal VMN GABAergic cell GAD and pAMPK responses to hypoglycemia by GPbb siRNA treatment bolster the notion that suppression of gluco-inhibitory GABAergic transmission involves glycogen-mediated impairment of local GABA cell energy state.

Evidence here for augmented corticosterone secretion following GPbb siRNA administration shows that GPbb-controlled glycogenolysis limits output of this counter-regulatory hormone under eu- and hypoglycemic conditions. Observations of parallel effects of GPbb knockdown on hypoglycemic patterns of VMN GABAergic transmission and corticosterone secretion support the need for further research to address the possibility that a causal relationship may link these responses to down-regulated GPbb gene expression. Current results show that neither GP siRNA caused a significant change in magnitude of hypoglycemic hyperglucagonemia. The prospect remains, however, that glucagon secretion may be governed by concurrent glycogenolytic action of both GP variants. Evidence here that intra-VMN GP siRNA administration did not alter GPbb or GPmm protein expression in other hypothalamic metabolic structures, for example, PVH, DMN, LHA or ARH supports the likelihood that observed effects of those knockdown treatments on corticosterone secretion are mediated by transmitter responses to GP gene knockdown within the confines of the VMN.

It should be perceived that the current research design does not rule out a probability that elevated circulating INS levels ensuing from *sc* injection may directly affect one or more experimental endpoints investigated here, aside from hypoglycemia per se. It remains to be determined if hyperinsulinemia may attenuate or amplify the impact of glucose deficiency on VMN nitroergic or GABAergic neuron energy sensor activity and neurotransmission during IHH. Glucocorticoid receptors (GRs) are expressed throughout the brain, which permits widespread effects of hypoglycemic hypercorticosteronemia on neural function. It is unclear at present if VMN NO or GABA nerve cells are directly sensitive to corticosterone or receive GR-controlled afferent input. However, the possibility that augmented GR stimulation during hypoglycemia may modify reactivity of these neurons to glucopenia cannot be discounted.

The VMN controls a broad array of functions, in addition to counter-regulatory hormone secretion, that cooperatively

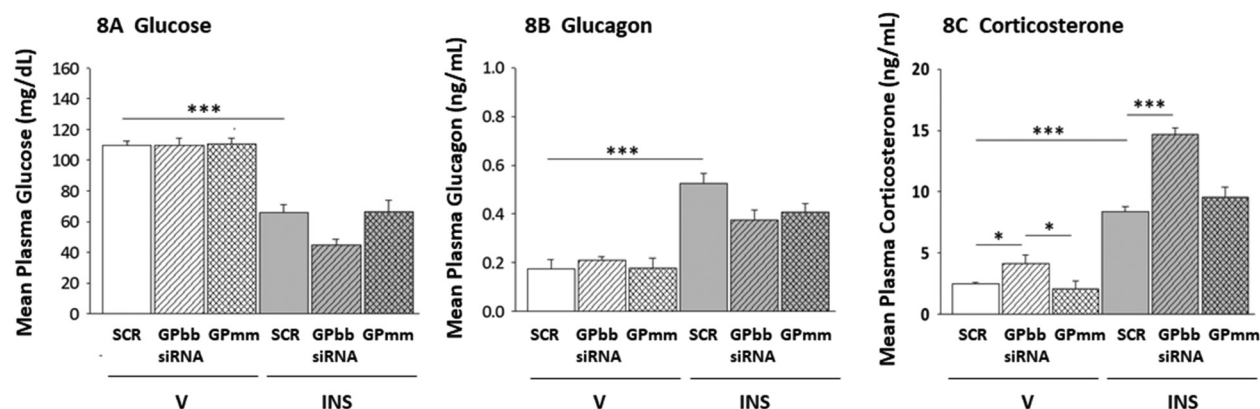


Figure 8. VMN GPbb versus GPmm regulation of plasma glucose concentrations and basal and hypoglycemia-associated patterns of counter-regulatory hormone secretion. Data show mean glucose (A), glucagon (B), and corticosterone (C) concentrations \pm SEM for the following treatment groups: SCR/V (solid white bars), GPbb siRNA/V (diagonal-striped white bars), GPmm siRNA/V (cross-hatched white bars), SCR/INS (solid gray bars), GPbb siRNA/INS (diagonal-striped gray bars), and GPmm siRNA/INS (cross-hatched gray bars). * $p < .05$; ** $p < .01$; *** $p < .001$.

Abbreviations: VMN = ventromedial hypothalamic nucleus; GP = glycogen phosphorylase; GPbb = glycogen phosphorylase-brain type; GPmm = glycogen phosphorylase-muscle type; SEM = standard error of mean; SCR = scramble; INS = insulin; V = vehicle; sc = subcutaneous.

maintain glucose homeostasis, including hepatic glucose production and peripheral glucose disposal (Shimazu & Minokoshi, 2017). The VMN stimulates liver gluconeogenesis, thereby augmenting circulating glucose levels, by parallel neural and endocrine (e.g., glucagon and epinephrine) mechanisms. VMN GI neurons are implicated in the latter function (Stanley et al., 2016), but their involvement in hepatic glucose output is unclear. On the other hand, VMN GE nerve cells govern peripheral glucose utilization (Toda et al., 2016) most likely via autonomic outflow (Shimazu & Minokoshi, 2017). Evidence from our work that VMN NO and GABA neurons express the hypoglycemia-activated energy gauge AMPK supports the notion that they function as first-order metabolic sensors. There remains a need to elucidate their respective contribution to neural regulation of peripheral glucose metabolism, and to clarify how glycogen metabolism may influence their control.

It should be noted that other ventromedial hypothalamic neurotransmitters, including glutamate, are implicated in neural control of glucose counter-regulation. Knockout of the neuron-specific vesicular glutamate transporter-2 was observed to suppress glucagon and epinephrine secretion and to inhibit hepatic gluconeogenic enzyme gene expression in the mouse (Tong et al., 2007). More recent work in rats shows that hypoglycemia-associated augmentation of ventromedial hypothalamic tissue glutamate levels is stimulatory to counter-regulatory hormone release through kainic acid receptor-dependent mechanisms (Chowdhury et al., 2017). Despite a current lack of proof that VMN glutaminergic neurons express AMPK, e.g. function as a first-order metabolic sensor, omission here of investigation of VMN GP variant regulation of baseline versus hypoglycemic patterns

of VMN-derived glutaminergic transmission was a missed opportunity, which will be pursued in future research.

The presence of GABAergic neurons in hypothalamic structures situated near the VMN raises the prospect that GABA release from afferent projections to the VMN may affect one or more experimental endpoints evaluated here, including counter-regulatory hormone secretion. Although the current experimental design did not include validation by a reporter that administered GP siRNAs were confined to the VMN, evidence that intra-VMN GP variant siRNA administration altered GPbb and GPmm expression in that site, but not in the PVN, DMN, LHA, or ARH supports the view that glycogen breakdown in those neighboring locations was unaffected by VMN GP knockdown. However, present outcomes do not mitigate the chance that genetic manipulation of VMN GP activity might affect, by as-yet-unknown mechanisms, the functional status of extra-VMN GABA neurons that innervate the VMN. The possibility that laser-cataapult microdissection samples of individual neurochemically characterized VMN nerve cell bodies may contain an-as-yet-undetermined number of GABAergic synaptic terminals positioned near GAD_{65/67}-ir-positive perikarya cannot be disregarded. The extent to which axonal GAD protein may be included, if at all, in such samples will require confirmation by electron microscopic ultrastructural-level immunocytochemical analysis of tissue located within the high precision circular laser track placed around individual cell bodies.

The GAD_{65/67} primary antibody used here detects a single band of 65–67 kDa molecular weight (MW) in lysates of VMN micropunch tissue (Uddin et al., 2020) and of laser-microdissected GAD-immunopositive VMN neurons

(Mahmood et al., 2020). The whole immunoblot in Panel B-V, Figure 1, verifies consistent detection of a sole band of predicted MW in VMN GAD-ir-positive somal sample lysates from each of the six treatment groups used in the current experimental design. However, it should be noted that definitive proof of specificity of this antiserum for detection of VMN nerve cell body GAD_{65/67} in situ, namely demonstrable lack of VMN cell body labeling in a GAD_{65/67} animal knockout model and replication of neuroanatomical patterns of nerve cell GAD mRNA expression as revealed by in-situ hybridization or single-cell reverse transcription polymerase chain reaction, is currently lacking. Thus, outcomes reported here should be evaluated with that critical limitation in mind, as the possibility that the current GAD antiserum may exhibit, in part, nonspecific behavior (resulting in labeling of neurons that do not express GAD), when applied to brain tissue sections cannot be discounted.

Our initial work focusing on the VMN involved pooling tissue or cell samples collected over the entire length of that structure, but subsequent incorporation of discriminative analysis of distinctive rostro-caudal segments raised the prospect of region-based functional heterogeneity. In recent work (Uddin et al., 2020), hypoglycemia was observed to elicit rostro-caudal region-specific changes in VMN GP variant protein profiles. Those findings were the impetus here to investigate whether genetic suppression of each GP isoform had similar or divergent effects on target protein profiles in NO or GABA neurons also acquired according to VMN segment. Indeed, current data disclose VMN segment-distinctive GP variant control of nitrenergic and GABAergic neuron function. Although acquisition, processing, and analysis of pure nerve cell populations from separate rostro-caudal segments of the VMN are labor-intensive, we perceive that it can be valuable for exposing functional diversity over the length of this nucleus, a concept that is bolstered by present results. The immense value of examination of dorsomedial, central, and ventrolateral divisions of the VMN is not disputed here. We consider that insight gained here on how glycogen metabolism impacts rostral, middle, versus caudal VMN populations of each neurotransmitter phenotype to provide a useful foundation to new investigate whether observed segment-specific protein responses to GP siRNA are derived from neurons located in all or a subset of those divisions within that segment.

In summary, current outcomes validate the efficacy of GP siRNA delivery for manipulation of glycogen breakdown in discrete brain structures in vivo, and provide novel evidence for divergent VMN GPbb regulation of GPmm expression during glucostasis versus neuro-glucopenia. Data identify locations within the VMN wherein GP variant-specific regulation of basal or hypoglycemic patterns of GABAergic and nitrenergic transmission occur. Change in direction of glycogenolytic control of metabolic-sensory neuron AMPK suggests that different indicators of glycogen metabolism may be monitored by these cells during energy stability versus imbalance.

Intensification of hypoglycemic stimulation of nitrenergic and GABAergic nerve cell pAMPK profiles by GPbb knockdown indicates that GP-mediated glycogen mobilization limits neuronal energy instability during hypoglycemia.



Declaration of Conflicting Interests

The authors declared no potential conflicts of interest with respect to the research, authorship, and/or publication of this article.

Funding

The authors disclosed receipt of the following financial support for the research, authorship, and/or publication of this article: This work was supported by the National Institutes of Health (grant no. DK 109382).

ORCID iDs

Mostafa M. H. Ibrahim  <https://orcid.org/0000-0003-2038-9933>
Karen P. Briski  <https://orcid.org/0000-0002-7648-1395>

References

- Ashford, M. L. J., Boden, P. R., & Treherne, J. M. (1990). Glucose-induced excitation of hypothalamic neurons is mediated by ATP-sensitive K⁺ channels. *Pflügers Arch*, *415*, 479–483. <https://doi.org/10.1007/bf00373626>.
- Bélangier, M., Allaman, I., & Magistretti, P. J. (2011). Brain energy metabolism: Focus on astrocyte-neuron metabolic cooperation. *Cell Metabol*, *14*, 724–738. <https://doi.org/10.1016/j.cmet.2011.08.016>.
- Briski, K. P., Ibrahim, M. M. H., Mahmood, A. S. M. H., & Alshamrani, A. A. (2021). Norepinephrine regulation of ventromedial hypothalamic nucleus astrocyte glycogen metabolism. *Int J Mol Sci*, *22*(2), E759. <https://doi.org/10.3390/ijms22020759>.
- Briski, K. P., Mandal, S. K., Bheemanapally, K., & Ibrahim, M. M. H. (2020). Effects of acute versus recurrent insulin-induced hypoglycemia on ventromedial hypothalamic nucleus metabolic-sensory neuron AMPK activity: Impact of alpha₁-adrenergic receptor signaling. *Brain Res Bull*, *157*, 41–50. <https://doi.org/10.1016/j.brainresbull.2020.01.013>.
- Briski, K. P., Marshall, E. S., & Sylvester, P. W. (2001). Effects of estradiol on glucoprivic transactivation of catecholaminergic neurons in the female rat caudal brainstem. *Neuroendocrinology*, *73*, 369–377. <https://doi.org/10.1159/000054655>.
- Bröer, S., Rahman, B., Pellegrini, G., Pellerin, L., Martin, J. L., Verleysdonk, S., Hamprecht, B., & Magistretti, P. J. (1997). Comparison of lactate transport in astroglial cells and monocarboxylate transporter 1 (MCT 1) expressing *Xenopus laevis* oocytes. Expression of two different monocarboxylate transporters in astroglial cells and neurons. *J Biol Chem*, *272*, 30096–30102. <https://doi.org/10.1074/jbc.272.48.30096>.
- Brown, A. M. (2004). Brain glycogen re-awakened. *J Neurochem*, *89*, 537–552. <https://doi.org/10.1111/j.1471-4159.2004.02421.x>.
- Butcher, R. L., Collins, W. E., & Fugo, N. W. (1974). Plasma concentrations of LH, FSH, progesterone, and estradiol-17beta throughout the 4-day estrous cycle of the rat. *Endocrinology*, *94*, 1704–1708. <https://doi.org/10.1210/endo-94-6-1704>.

- Chan, O., Zhu, W., Ding, Y., McCrimmon, R. J., & Sherwin, R. S. (2006). Blockade of GABA(A) receptors in the ventromedial hypothalamus further stimulates glucagon and sympathoadrenal but not the hypothalamo-pituitary-adrenal response to hypoglycemia. *Diabetes*, *55*, 1080–1087. <https://doi.org/10.2337/diabetes.55.04.06.db05-0958>.
- Chowdhury, G. M. I., Wang, P., Ciardi, A., Mamillapalli, R., Johnson, J., Zhu, W., Eid, T., Behar, K., & Chan, O. (2017). Impaired glutamatergic neurotransmission in the ventromedial hypothalamus may contribute to defective counterregulation in recurrently hypoglycemic rats. *Diabetes*, *66*, 1979–1989. <https://doi.org/10.2337/db16-1589>.
- Cryer, P. E. (2015). Hypoglycemia-associated autonomic failure in diabetes: Maladaptive, adaptive, or both? *Diabetes*, *64*, 2322–2323. <https://doi.org/10.2337/db15-0331>.
- Cryer, P. E. (2017). Individualized glycemic goals and an expanded classification of severe hypoglycemia in diabetes. *Diabetes Care*, *40*, 1641–1643. <https://doi.org/10.2337/dc16-1741>.
- Fioramonti, X., Marsollier, N., Song, Z., Fakira, K. A., Patel, R. M., Brown, S., Duparc, T., Pica-Mendez, A., Sanders, N. M., Knauf, C., Valet, P., McCrimmon, R. J., Beuve, A., Magnan, C., & Routh, V. H. (2010). Ventromedial hypothalamic nitric oxide production is necessary for hypoglycemia detection and counter-regulation. *Diabetes*, *59*, 519–528. <https://doi.org/10.2337/db09-0421>.
- Gruetter, R. (2003). Glycogen: The forgotten cerebral energy store. *J Neurosci Res*, *74*, 179–183. <https://doi.org/10.1002/jnr.10785>.
- Han, S. M., Namkoong, C., Jang, P. G., Park, I. S., Hong, S. W., Katakami, H., Chun, S., Kim, S. W., Park, J. Y., Lee, K. U., & Kim, M. S. (2005). Hypothalamic AMP-activated protein kinase mediates counter-regulatory responses to hypoglycaemia in rats. *Diabetologia*, *48*, 2170–2178. <https://doi.org/10.1007/s00125-005-1913-1>.
- Ibrabim, M. M. H., Bheemanapally, K., Alhamami, H. N., & Briski, K. P. (2020). Effects of intracerebroventricular glycogen phosphorylase inhibitor CP-316,819 infusion on hypothalamic glycogen content and metabolic neuron AMPK activity and neurotransmitter expression in the male rat. *J Mol Neurosci*, *70*, 647–658. <https://doi.org/10.1007/s12031-019-01471-0>.
- Ibrahim, M. M. H., Alhamami, H. N., & Briski, K. P. (2019). Norepinephrine regulation of ventromedial hypothalamic nucleus metabolic transmitter biomarker and astrocyte enzyme and receptor expression: Impact of 5'-AMP-activated protein kinase. *Brain Res*, *1711*, 48–57. <https://doi.org/10.1016/j.brainres.2019.01.012>.
- Laming, P., Kimelberg, H., Robinson, S., Salm, A., Hawrylak, N., Müller, C., Roots, B., & Ng, K. (2000). Neuronal–glial interactions and behavior. *Neurosci Biobehav Rev*, *24*, 295–340. [https://doi.org/10.1016/s0149-7634\(99\)00080-9](https://doi.org/10.1016/s0149-7634(99)00080-9).
- López, M. (2018). Hypothalamic AMPK and energy balance. *Eur J Clin Invest*, *48*, e12996. <https://doi.org/10.1111/eci.12996>.
- Mahmood, A. S. M. H., Napit, P. R., Ali, M. H., & Briski, K. P. (2020). Estrogen receptor involvement in noradrenergic regulation of ventromedial hypothalamic nucleus glucoregulatory neurotransmitter and stimulus-specific glycogen phosphorylase enzyme isoform expression. *ASN Neuro*, *12*, 1759091420910933. <https://doi.org/10.1177/1759091420910933>.
- Mandal, S. K., Shrestha, P. K., Alenazi, F. S. H., Shakya, M., Alhamami, H. N., & Briski, K. P. (2017). Role of hindbrain adenosine 5'-monophosphate-activated protein kinase (AMPK) in hypothalamic AMPK and metabolic neuropeptide adaptation to recurring insulin-induced hypoglycemia in the male rat. *Neuropeptides*, *66*, 25–35. <https://doi.org/10.1016/j.npep.2017.08.001>.
- Mandal, S. K., Shrestha, P. K., Alenazi, F. S. H., Shakya, M., Alhamami, H. N., & Briski, K. P. (2018). Effects of estradiol on lactoprovic signaling of the hindbrain upon the contraregulatory hormonal response and metabolic neuropeptide synthesis in hypoglycemic female rats. *Neuropeptides*, *70*(70), 37–46. <https://doi.org/10.1016/j.npep.2018.05.004>.
- McCrimmon, R. J., Shaw, M., Fan, X., Cheng, H., Ding, Y., Vella, M. C., Zhou, L., McNay, E. C., & Sherwin, R. S. (2008). Key role for AMP-activated protein kinase in the ventromedial hypothalamus in regulating counterregulatory hormone responses to acute hypoglycemia. *Diabetes*, *57*, 444–450. <https://doi.org/10.2337/db07-0837>.
- Müller, M. S., Pedersen, S., Walls, A. B., Waagepetersen, H. S., & Bak, L. K. (2014). Isoform-selective regulation of glycogen phosphorylase by energy deprivation and phosphorylation in astrocytes. *Glia*, *63*, 154–162. <https://doi.org/10.1002/glia.22741>.
- Nadeau, O. W., Fontes, J. D., & Carlson, G. M. (2018). The regulation of glycogenolysis in the brain. *J Biol Chem*, *293*, 7099–7107. <https://doi.org/10.1074/jbc.r117.803023>.
- Napit, P. R., Ali, M. H., Shakya, M., Mandal, S. K., Bheemanapally, K., Mahmood, A. S. M. H., Ibrahim, M. M. H., & Briski, K. P. (2019). Hindbrain estrogen receptor regulation of counter-regulatory hormone secretion and ventromedial hypothalamic nucleus glycogen content and glucoregulatory transmitter signaling in hypoglycemic female rats. *Neuroscience*, *411*, 211–221. <https://doi.org/10.1016/j.neuroscience.2019.05.007>.
- Obel, L. F., Müller, M. S., Walls, A. B., Sickmann, H. M., Bak, L. K., Waagepetersen, H. S., & Schousboe, A. (2012). Brain glycogen—new perspectives on its metabolic function and regulation at the subcellular level. *Front Neuroenerget*, *4*, 3. <https://doi.org/10.3389/fnene.2012.00003>.
- Oomura, Y., Ono, H., Ooyama, H., & Wayner, M. J. (1969). Glucose and osmosensitive neurons of the rat hypothalamus. *Nature*, *222*, 282–284. <https://doi.org/10.1038/222282a0>.
- Pimentel, G. D., Ropelle, E. R., Rocha, G. Z., & Carvalheira, J. B. (2013). The role of neuronal AMPK as a mediator of nutritional regulation of food intake and energy homeostasis. *Metabolism*, *62*, 171–178. <https://doi.org/10.1016/j.metabol.2012.07.001>.
- Routh, V. H., Hao, L., Santiago, A. M., Sheng, Z., & Zhou, C. (2014). Hypothalamic glucose sensing: Making ends meet. *Front Syst Neurosci*, *8*, 236. <https://doi.org/10.3389/fnsys.2014.00236>.
- Schousboe, A., Sickmann, H. M., Walls, A. B., Bak, L. K., & Waagepetersen, H. S. (2010). Functional importance of the astrocyte glycogen shunt and glycolysis for maintenance of an intact intra/extracellular glutamate gradient. *Neurotox Res*, *18*, 94–99. <https://doi.org/10.1007/s12640-010-9171-5>.
- Shimazu, T., & Minokoshi, T. (2017). Systemic glucoregulation by glucose-sensing neurons in the ventromedial hypothalamic nucleus (VMN). *J Endocr Soc*, *1*(5), 449–450. <https://doi.org/10.1210/js.2016-1104>.** Journal of the Endocrine Society *** 449–459.
- Shulman, R. G., Hyder, F., & Rothman, D. L. (2001). Cerebral energetics and the glycogen shunt: Neurochemical basis of functional imaging. *Proc Natl Acad Sci*, *98*, 6417–6422. <https://doi.org/10.1073/pnas.101129298>.

- Silver, I. A., & Erecińska, M. (1998). Glucose-induced intracellular ion changes in sugar-sensitive hypothalamic neurons. *J Neurophysiol*, *79*, 1733–1745. <https://doi.org/10.1152/jn.1998.79.4.1733>.
- Stanley, S. A., Kelly, L., Latcha, K. N., Schmidt, S. F., Yu, X., Nectow, A. R., Sauer, J., Dyke, J. P., Dordick, J. S., & Friedman, J. M. (2016). Bidirectional electromagnetic control of the hypothalamus regulates feeding and metabolism. *Nature*, *531*(7596), 647–650. <https://doi.org/10.1038/nature17183>
- Stobart, J. L., & Anderson, C. M. (2013). Multifunctional role of astrocytes as gatekeepers of neuronal energy supply. *Cell Neurosci*, *7*, 1–21. <https://doi.org/10.3389/fncel.2013.00038>.
- Suzuki, H., Hagegawa, Y., Kanawaru, K., & Zhang, J. H. (2010). Mechanisms of osteopontin-induced stabilization of blood-brain barrier disruption after subarachnoid hemorrhage in rats. *Stroke*, *41*, 1783–1790. <https://doi.org/10.1161/strokeaha.110.58653>.
- Toda, C., Kim, J. D., Impellizzeri, D., Cuzzocrea, S., Liu, Z.-W., & Diano, S. (2016). UCP2 regulates mitochondrial fission and ventromedial nucleus control of glucose responsiveness. *Cell*, *164*(5), 872–883. <https://doi.org/10.1016/j.cell.2016.02.010>
- Tong, Q., Ye, C., McCrimmon, R. J., Dhillon, H., Choi, B., Kramer, M. D., Yu, J., Yang, Z., Christiansen, L. M., Lee, C. E., Choi, C. S., Zigman, J. M., Shulman, G. I., Sherwin, R. S., Elmquist, J. K., & Lowell, B. B. (2007). Synaptic glutamate release by ventromedial hypothalamic neurons is part of the neurocircuitry that prevents hypoglycemia. *Cell Metab*, *5*, 383–393. <https://doi.org/10.1016/j.cmet.2007.04.001>.
- Uddin, M. M., Bheemanapally, K., Ibrahim, M. M. H., & Briski, K. P. (2020). Sex-dimorphic neuroestradiol regulation of ventromedial hypothalamic nucleus glucoregulatory transmitter and glycogen metabolism enzyme protein expression in the rat. *BMC Neurosci*, *21*(1), 51. <https://doi.org/10.1186/s12868-020-00598-w>.
- Uddin, M. M., Mahmood, A. S. M. H., Ibrahim, M. M. H., & Briski, K. P. (2019). Sex dimorphic estrogen receptor regulation of ventromedial hypothalamic nucleus glucoregulatory neuron adrenergic receptor expression in hypoglycemic male and female rats. *Brain Res*. <https://doi.org/10.1016/j.brainres.2019.146311>.
- Xue, B., & Kahn, B. B. (2006). AMPK integrates nutrient and hormonal signals to regulate food intake and energy balance through effects in the hypothalamus and peripheral tissues. *J Physiol*, *574*, 73–83. <https://doi.org/10.1113/jphysiol.2006.113217>.